energies

MDPI

Article

Design of a Low-Cost Electrostatic Precipitator to Reduce Particulate Matter Emissions from Small Heat Sources

Juraj Drga [1], Michal Holubčík [1,*], Nikola Čajová Kantová [2] and Bystrík Červenka [1]

[1] Department of Power Engineering, Faculty of Mechanical Engineering, University of Žilina, Univerzitna 1, 010 26 Zilina, Slovakia; juraj.drga@fstroj.uniza.sk (J.D.); bystrik.cervenka@fstroj.uniza.sk (B.Č.)
[2] Research Centre, University of Žilina, Univerzitna 1, 010 26 Zilina, Slovakia; nikola.cajovakantova@uniza.sk
* Correspondence: michal.holubcik@fstroj.uniza.sk

Abstract: Capturing particulate matter (PM) is an important issue due to the protection of human health and the quality of their life. This paper describes the innovation of an affordable particulate matter capture device for small heat sources to reduce particulate matter emissions. The design of two investigated variants of the device is based on the principle of a tubular electrostatic precipitator with one charging electrode placed in the chimney. The design of the precipitators is aimed at increasing the area of the collecting electrodes by elements dividing precipitation space, with a simultaneously increased number of charging electrodes. The influence of the elements' application on the pressure drop and the gas flow velocity through the devices is analyzed by computational fluid dynamics (CFD). The work is further focused on the economic evaluation of precipitators and design adjustments for lower energy consumption. The achieved results show the right direction of efforts to improve the equipment designed to capture PM emissions.

Keywords: particulate matter; emissions; electrostatic precipitation; corona discharge; small heat sources; computational fluid dynamics

Citation: Drga, J.; Holubčík, M.; Čajová Kantová, N.; Červenka, B. Design of a Low-Cost Electrostatic Precipitator to Reduce Particulate Matter Emissions from Small Heat Sources. *Energies* **2022**, *15*, 4148. https://doi.org/10.3390/en15114148

Academic Editor: Pouya Ifaei

Received: 29 April 2022
Accepted: 2 June 2022
Published: 5 June 2022

1. Introduction

Particulate matter (PM) is a major component of air pollution. Its high concentration negatively affects the cardiovascular system and can lead to respiratory and other diseases that significantly affect the quality and duration of human life [1–3]. Although the production of PM emissions is steadily decreasing, especially in the fields of industrial production and transportation, as shown in Figure 1, the field of heating with small heat sources in households is lagging far behind. Large-chamber electrostatic precipitators have already gained acceptance in the industry [4], and their principle ensures the high efficiency of fine dust collection. Studies have also been conducted on the electrostatic precipitation of PM from diesel vehicles [5–7]. We believe that electrostatic precipitators are an important prospect for the ecological future. Combined with low-polluting fuels, they can compete with alternative heating methods, which are increasingly used in modern society [8]. This work deals with the development of a tubular electrostatic precipitator that will be suitable for connection to a small solid fuel heat source. The importance of this topic is mainly due to the fact that the production of PM emissions in households is much higher, by about 62.9% for PM10 and 79% for PM2.5 [9] than in other emission producing sectors. Legislation that would lead to a reduction in PM emissions from households is expected to be changed soon. Therefore, there is a great potential for the capture of particulate matter using a tubular electrostatic precipitator.

The principle of the precipitator is to connect the collecting and discharging electrodes to a high voltage source DC. The collecting electrode may consist of a chimney tube made of metal and is connected to the positive pole of the HV voltage source. The discharge electrode may be formed by a wire-shaped or otherwise spiked conductor connected to the negative terminal of the voltage source. A corona discharge is generated on such a

conductor when a sufficient supply voltage is applied. At the same time, the electrodes are separated by insulators and the collecting electrode is grounded. The level of the applied voltage affects the operation of the device. If the value of the critical initial voltage is exceeded, a corona discharge begins to form at the discharge electrode, and the gas is ionized in the ionization region near the electrode. Here, weakly bound electrons begin to be released and continue to migrate into the transport region, simultaneously forming positive ions in the ionization region. The transport region is located beyond the ionization region, which in contrast, has a larger area. PM binds free electrons together In this region because they are predominantly carbon, which is an electronegative element. In this way, negative ions are formed by the combination of neutral solid particles and free electrons, which are attracted by electrical forces to the positively charged precipitation electrode. The charged particles are deposited on the electrode and do not disintegrate into particles of the original size even during cleaning but remain collected in clusters. The efficiency of such devices is influenced, for example, by the dimensions of the electrodes, the size of the deposition surface of the precipitator, the magnitude of the voltage applied, the velocity of the flowing gas, and the number of particles deposited on the precipitation electrode, etc.

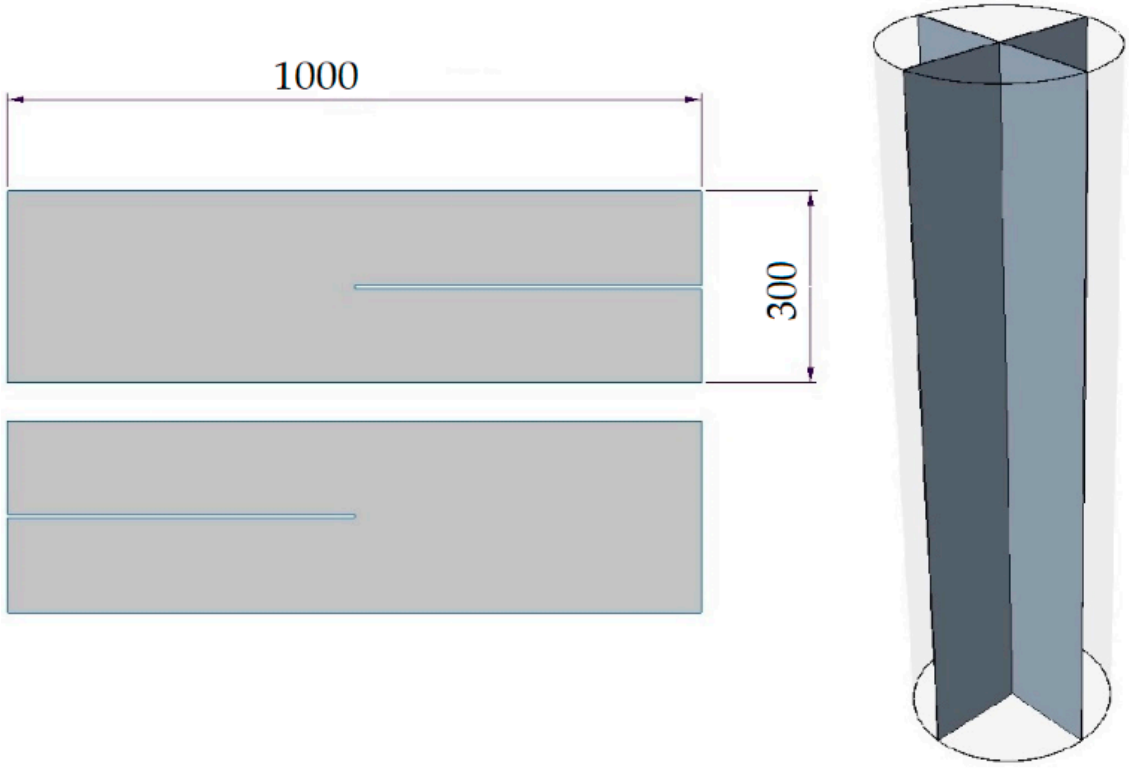

Figure 1. Sheet metal partition model.

The aim of this work is to create an efficient device suitable for heating households with solid fuel, while the focus is on price and operational affordability. Inspiration comes from the development of a precipitator with four collecting pipes placed in a chimney [10]. It was possible to achieve a separation level up to 85% with a precipitator length of 2 m and a preliminary improved variant of the tubular precipitator. The aim of this work is to innovate the equipment to achieve greater efficiency of PM capture. Compared to other developed precipitators, the target is to achieve progress by increasing the collector area by optimizing the collecting electrodes. The simple principle of a tubular precipitator is innovated by dividing the cross-section into four equal chambers, with a charging electrode in each. More than a twofold increase in the collection area while maintaining the external dimensions of the device is achievable with such construction. The primary purpose of this paper is to compare the new design with the previous concept of electrostatic precipitation.

The new concept envisions the collecting electrode as a cruciform metal sheet partition inserted into the chimney.

Several papers have been devoted to the topic of electrostatic precipitators in the past, examining proprietary prototypes or commercially available precipitators. Y. S. Eom performed a simulation of a chamber separator with a double-walled facade, finding that the efficiency of the separator was almost 93% at an inlet air velocity of 0.5 $m \cdot s^{-1}$ [11]. Xiang Gao built an experimental precipitator to study the effects of applied voltage, flow velocity, and temperature on the separation process., they a separation efficiency of 50–75% was achieved in [12] with different operating settings. Another experimental precipitator was dealt with by the work of Molchanov, which differed from the other devices in that it was placed directly in the combustion furnace. An efficiency of 56% was measured at the rated power of the heat source and 67% at a reduced power [13]. Carroll compared two types of commercial Schrader Al-Top ESP and OekoTube ESP. These were precipitators placed at the top of the chimney. The study reports achieving the precipitators efficiencies above 70% during automatic cleaning operations. Though, mechanical chimney cleaning would not guarantee higher efficiencies in the long run. The efficiency level was influenced by the type of fuel used, while the high costs were characterized by the highest concentration of emissions [14]. The OekoTube ESP precipitator was also part of Brunner's work, which involved two years of monitoring the operation of three electrostatic precipitators used on old wood-fired heating systems. The measurement results showed that these devices are suitable for older heat sources and could achieve an efficiency between 80.2 and 97.7% [15].

An important part of the work is a numerical simulation, based on which it is possible to predict important parameters of the device. Numerical simulations have already been carried out by M. Ahmadi1 [16], S. Haque [17], L. Zhao [18], G. Skodras [19], Akinori Zukeran [20], Keping Yan [21], A. Mohebbi [22], and Baoyu Guo [23], who have studied the distribution of the electric field, the trajectory of the PM, the number of trapped particles, etc., utilizing 2D CFD models. The shape of the charging electrode is designed, which affects the charging process in the precipitator. Investigation of the CFD simulation results enabled the shape of the discharge electrode optimization, which enables the required parameters for particle charging. Such simulations have already been performed by Xiufeng Guo [24], R.C. Everson [25], and Ming Dong [26,27].

2. Materials and Methods

The electrostatic precipitator, which was investigated, consists of two constructions. To extend the principle of a classical tubular precipitator with an ionization electrode, and the first version is based on the work carried out by our department [10]. In this case, the authors added a precipitator into the original 200 mm diameter chimney tube, which consisted of an extended 300 mm tube containing four smaller 120 mm tubes representing the precipitation electrodes. This allowed the collection area of the precipitator to be increased. Four ionization electrodes were guided in them. The precipitator was connected to 200 mm diameter chimneys at both ends via reducers. In the second construction of the separator, replace four pipes with a diameter of 120 mm with a cross-shaped metal sheet template, as shown in Figure 1. The aim is to eliminate the blind space between the 120 mm pipes created by this application. The collection area of the precipitator, which is composed of the area of the 300 mm chimney and the area of the cross-shaped sheet metal partition, becomes even larger. A comparison of the sizes of the collection areas is shown in Table 1. There are the following important parameters of the device in addition to the collection area, including the diameter of the collection electrodes, the diameter of the charging electrodes or the cross-section of the separator, etc. As the diameter of the charging electrodes increases, the value of the critical initial voltage for the start of corona discharge increases.

Table 1. Comparison of collecting areas of different types of precipitators.

Length of Precipitator 1 m	Collecting Area [m^2]
Tubular precipitator with 1 ionization electrode and 1 collecting electrode Ø = 300 mm	0.94
Tubular precipitator with 4 ionization electrodes and 4 collecting tubes Ø = 120 mm	1.51
Tubular precipitator with 4 ionization electrodes and 1 collecting electrode Ø = 300 mm with cross-shaped partition	2.14

Figure 2 shows the geometry of the two precipitators. A part of Figure 2a represents a variant with four collecting pipes 120 mm. The outer tube has a diameter of 300 mm, and the length of the precipitator is assumed to be 1 m in this work. The ionization electrodes are represented by four M4 threaded rods, which ensure sufficient strength of the structure. They are connected by a metal cross to which a DC is connected. The construction of the ionization electrodes is isolated from the collection tubes by ceramic inserts located at the top and bottom of the collection tubes. There is also a ceramic insert below the collection tubes, which serves as a base for the tubes to hold the system in place against downward displacement. Part of Figure 2b shows the geometry of the precipitator with a cross-shaped collection wall that touches the inner wall of the chimney at the edges. This variant differs from the previous one only in the attachment of the partition. All other parts of the system remain the same.

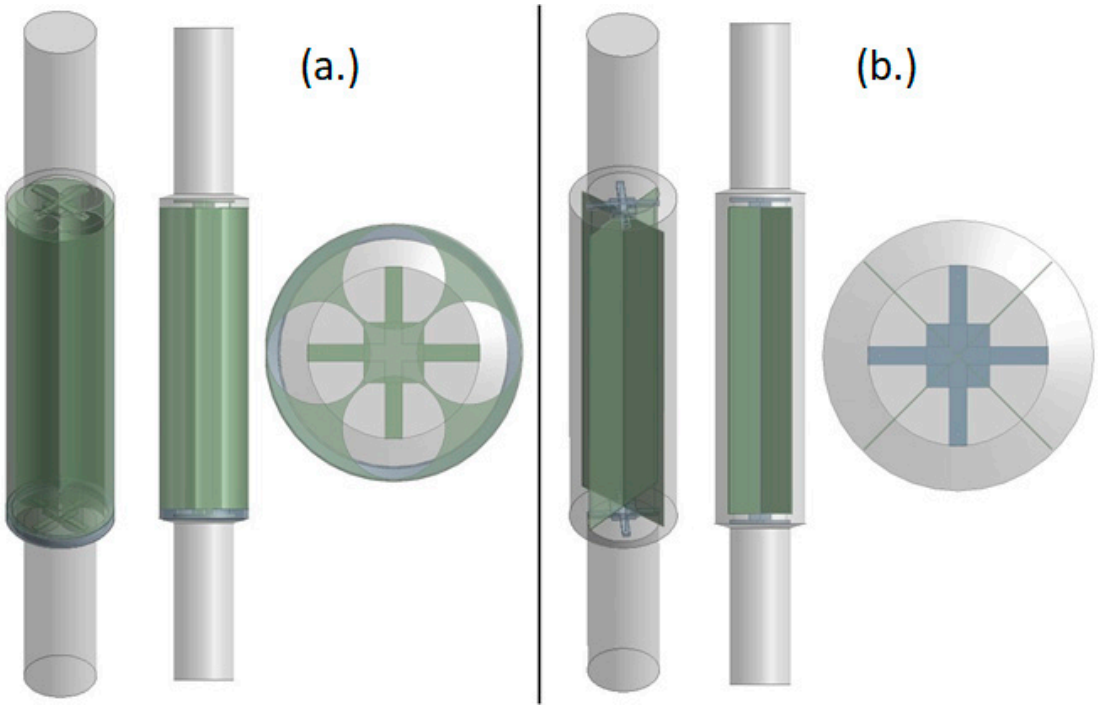

Figure 2. Geometry of precipitators: (**a**) variant with four collecting electrodes; (**b**) variant with a cross-shaped collecting partition.

The CX-600A power supply is a high voltage source whose advantage is affordability. The high voltage output is adjustable 5–60 kV, with a rated current of 3–5 mA. These parameters are sufficient for the application in the given devices. The device still has the function of constant and intermittent pulse mode, but it is unsuitable for the operation of the separator. The device is shown in Figure 3.

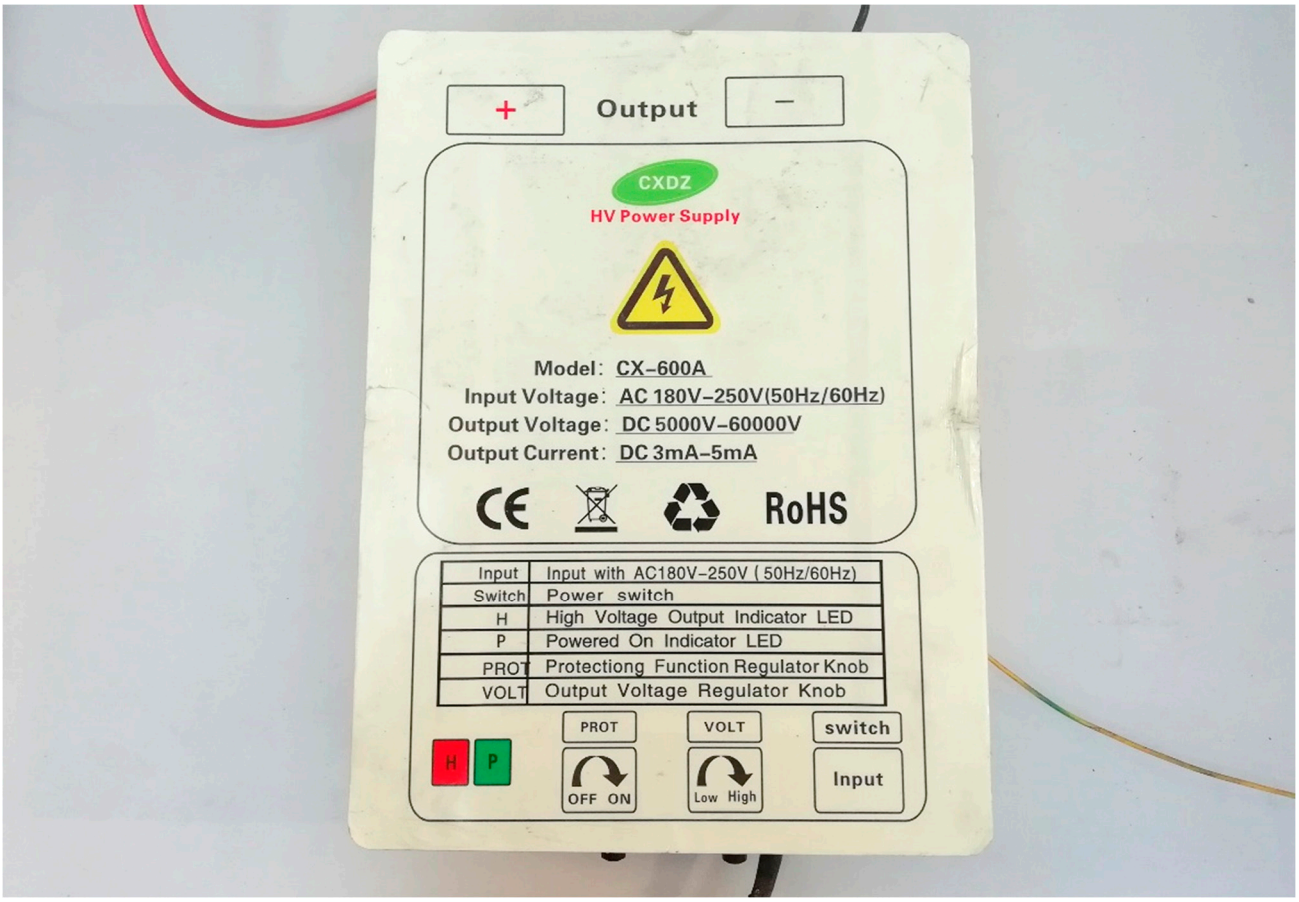

Figure 3. HV DC supply for precipitators.

Numerical Calculation

The basic parameters of the precipitator were calculated based on the available literature [28]. The calculations were performed based on a tubular precipitator with a circular cross-section, which corresponds to the variant with 120 mm collection tubes. Based on the proposed system dimensions, it was possible to calculate the capacity of the precipitator, the initial critical field strength, the initial critical voltage, and the radius of the ionization region. The calculated parameters for the precipitation section with a diameter of 120 mm are shown in Table 2.

Table 2. Calculated parameters of the precipitator.

Quantity	Calculated Value
C	6.55×10^{-11} F
E_{0c}	5.23×10^{6} V·m^{-1}
U_{0c}	3.56×10^{4} V
z (at a supply voltage of 40 kV)	2.31×10^{-3} m

The capacity of the precipitator was calculated according to Equation (1).

$$C = \frac{\varepsilon_0 \varepsilon_1 A}{R \ln\left(\frac{R}{r}\right)} \text{ [F]} \quad (1)$$

where ε_0 is the dielectric constant of the vacuum, ε_1 is the relative dielectric constant of the gas, A is the collection area, R is the radius of the collection electrode, and r is the radius of the discharge electrode.

The critical initial field strength was calculated according to Equation (2).

$$E_{0c} = k_1 \vartheta \left[1 + \frac{k_2}{\sqrt{(\vartheta r)}}\right] \left[\mathrm{V \cdot m^{-1}}\right] \quad (2)$$

where k_1, k_2 are quantities of the Whitehead–Brown equation, ϑ is the relative gas density.

The critical initial voltage was calculated according to Equation (3).

$$U_{0c} = r\, E_{0c} \ln\left(\frac{R}{r}\right) [\mathrm{V}] \quad (3)$$

The radius of the ionization region at pure gas was calculated according to Equation (4).

$$z = \frac{1}{2\vartheta}\left[\frac{2U}{k_1 ln\left(\frac{R}{r}\right)} + k_2^2 - k_2\sqrt{\left(\frac{4U}{k_1 ln\left(\frac{R}{r}\right)} + k_2^2\right)}\right] [\mathrm{m}] \quad (4)$$

where U is the applied voltage. Table 2 shows the calculated parameters of the precipitator.

3. Results and Discussion

3.1. CFD Simulation

CFD simulations of gas flow through models of the proposed devices were performed using Ansys Fluent software in order to visualize the pressure drop and gas flow rate of the precipitators. The models consisted of precipitators with a length of 1 m and 0.5 m piping upstream and downstream of the precipitator as inlet and outlet. The mesh of the model with the collection tubes consisted of 230,970 tetrahedral cells, while the model with the sheet metal partition consisted of 209,360 cells. The quality of the mesh was considered adequate based on an average value of the orthogonal quality at 0.56, the skewness at 0.36, and the aspect ratio at 1.42. The simulation was based on the k-omega SST turbulence model without discrete phase injection. In terms of boundary conditions, the inlet velocity of 1 m/s was applied at the inlet. The outlet was defined as a pressure outlet with a gauge pressure of −12 Pa for the simulation of the stack draft. Turbulence was defined as 5% for turbulent backflow intensity and 10 for turbulent backflow turbulent viscosity ratio for both inlet and outlet. The boundaries of precipitators were defined as stationary walls with no-slip shear conditions.

Figure 4 shows the resulting pressure field for both types of precipitators. The pressure drop of the precipitator with four collection tubes was about 1.5 Pa. As can be seen from Figure 4, the pressure drop in the precipitators changes only slightly, in the range of 0.1 Pa. For the variant with a partition precipitator, the pressure drop is reduced by about 8%.

Figure 5 shows the distribution of the gas flow rate through the precipitators. A decrease in velocity can be observed in the precipitation space in the partition precipitator, which is suitable for the precipitation process. There is flow velocity reduction from 0.91 $\mathrm{m \cdot s^{-1}}$ to 0.89 $\mathrm{m \cdot s^{-1}}$ within the first third of the precipitation space. In the middle part of the precipitation space, the velocity already decreased from 0.73 $\mathrm{m \cdot s^{-1}}$ to 0.52 $\mathrm{m \cdot s^{-1}}$. A decrease in the mean velocity from 0.72 $\mathrm{m \cdot s^{-1}}$ to 0.48 $\mathrm{m \cdot s^{-1}}$ s was predicted in the last upper third of the space.

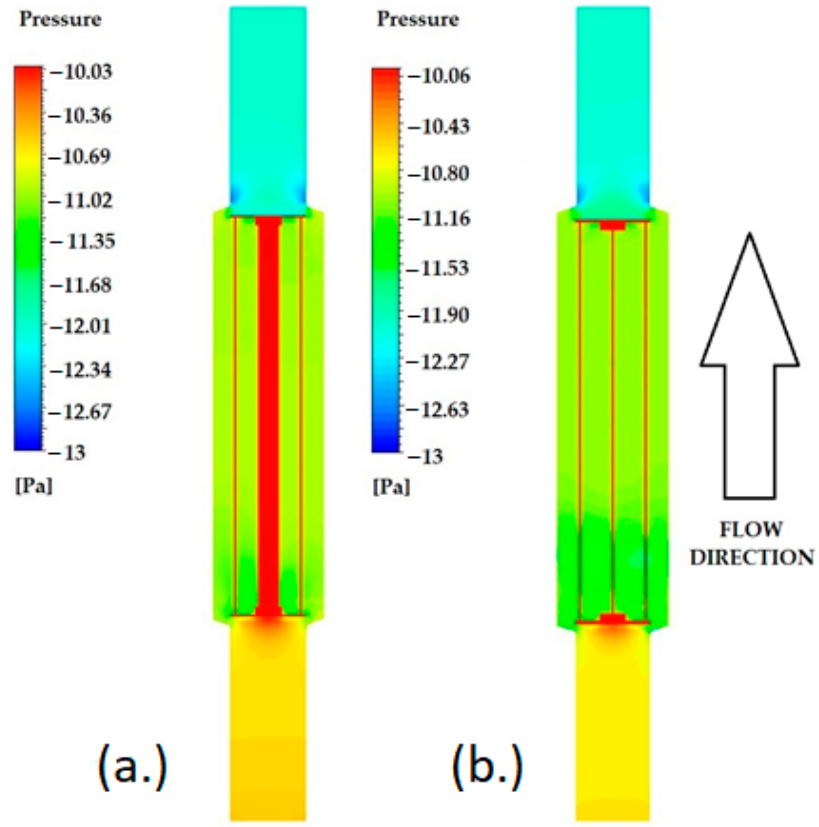

Figure 4. The simulated pressure in (**a**) variant with four collecting electrodes; (**b**) variant with a cross-shaped collecting partition.

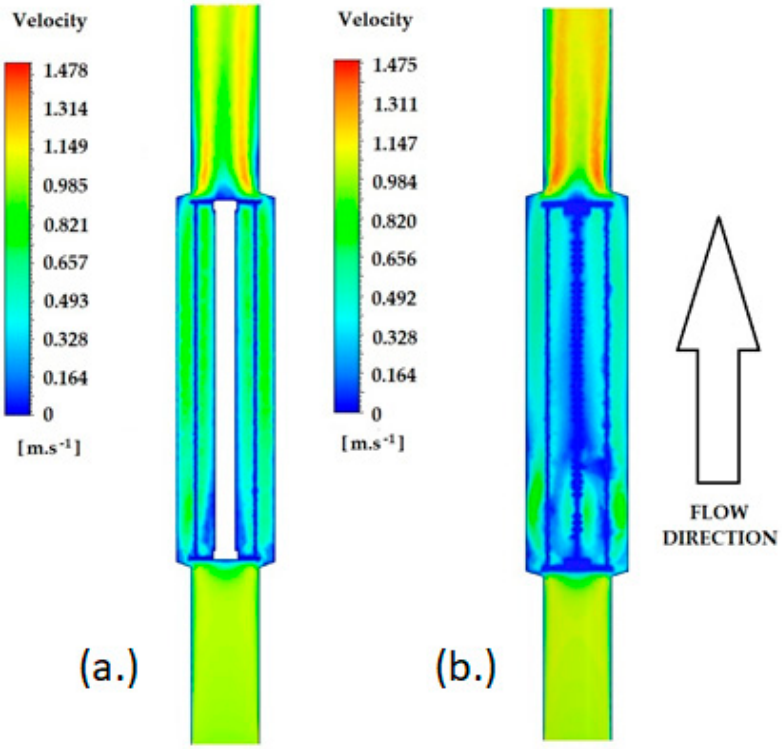

Figure 5. The simulated velocity in (**a**) variant with four collecting electrodes; (**b**) variant with a cross-shaped collecting partition.

3.2. Economic Evaluation

As mentioned above, our goal is to develop an efficient device for electrostatic precipitation of PM from small heat sources. The focus is on the low investment cost of procurement, which would facilitate the widespread adoption of such a measure to improve air quality. Due to the current world situation and the constant increase in the prices of basic necessities and energy, the population does not have sufficient funds for such investments. If one wished to deepen the theoretical discussion, it would be necessary to consider the financial support of the population by the states, which could lead to a greater interest in such facilities. At the same time, an educational campaign on the proper combustion of fuels and the use of appropriate fuels with lower emissions that ultimately affect their production would be useful [29,30].

Table 3 shows the economic cost of purchasing electrostatic precipitators. The advantage of these devices, as mentioned earlier, is the possibility of connecting an electrostatic precipitator to older combustion devices [7]. This enables cost saving for the consumer without avoiding the purchase of a new heat source. To the estimated total price of the device, we calculated the approximate annual operating costs of the power supply HV at 400 W (maximum wattage specified by the manufacturer at a voltage of 40 kV) with an average daily operating time of 7 h during the heating season (the number of heating days was set at about 220 days) with an average price of 0.16 €/1 kWh. Under these conditions, the annual operating costs are 94 €. With a pellet boiler, including the precipitator, the annual heating costs increase to 500 € (together with the annual fuel and maintenance costs), which is about 30 € less than the annual operating costs of the heat pump and 50 € more than burning natural gas [31]. It is believed that such a choice is friendly for consumers while saving costs by optimizing an older functional heat source, at the expense of buying a modern plant with low PM production and a price of about 5000 €.

Table 3. The summary of the economic costs of procuring the device (CAPEX).

Item	Quantity	Price in €
Chimney pipe Ø = 300 mm	1	80
Chimney pipe Ø = 120 mm	4	30
Reduction 200/300	2	50
Threaded rod M4	4	8
Connecting material	-	40
High DC voltage source	1	200
Ceramic insulators	4	50
Total estimated price in € (procurement of equipment) *		**458**

* Without the annual cost of operating the HV source.

3.3. Possibilities of Modification of Proposed Devices

Several design adjustments are required to achieve higher efficiency of particle filtration. One of them is the optimization of the discharge electrode or its shape. The threaded rod guarantees the strength of the geometry, but due to the large diameter of the electrodes, a higher voltage must be applied for the capturing process. The smaller the electrode diameter, the lower the value of the initial critical voltage and the power of the voltage source. The way of modifying the discharge electrode, which is already widely used in practice, is to design it with a shape that produces peaks or thin protrusions that narrow the diameter of the electrode at certain points and create better conditions for the formation of a corona discharge [25,26]. The focus is on the design of a sheet metal discharge electrode containing such tips. This could be an acceptable solution from the production point of view, as well as from the price point of view. The second aspect that would enable a stable deposition process is the development of an automatic cleaning system. As the thickness of the deposited PM layer on the collecting electrodes increases, the deposition efficiency

decreases and can lead to a back corona in case of emergency. A rotating brush is not a suitable option in this case [32], as the stress on the chimney system in case of impact would have to be considered in the design of the rapping device. The focus is thus on the development of devices that are effective with low stress on the design of the precipitator and the chimney system, not least in terms of operation.

4. Conclusions

The core of our work is to increase the efficiency of PM capture by electrostatic precipitation to extend the basic principle of the in-chimney tubular precipitator with one discharging electrode to four precipitation chambers. The first design is based on a concept that had already been built in the institution. Four smaller diameter tubes were attached to the outer chimney, each with a discharging electrode. With such a design, the collection area of the precipitator could be increased by about 60%. However, a space was created between the smaller tubes where the precipitation process did not occur. To eliminate this "blind" space we used a sheet metal partition, which is the essence of the new design of the precipitator. This variant allows for an increase in the collection area of approximately 127% compared to a conventional precipitator with one discharging electrode and approximately 42% compared to a precipitator with four collecting electrodes.

The numerical simulations of both designs were then developed, focusing on the pressure drop and gas flow rates through the precipitators. The results showed that the pressure drop decreased minimally, by about 8%, when the partition was applied. However, the flow rate in the separation space has changed more significantly. In the first third of the separation space, the flow rate of the precipitator with partition decreased slightly from 0.91 $m \cdot s^{-1}$ to 0.89 $m \cdot s^{-1}$. In the middle section of the separation space, the velocity already decreased from 0.73 $m \cdot s^{-1}$ to 0.52 $m \cdot s^{-1}$. In the last, upper third of the separation space, the highest velocity change was calculated from 0.72 $m \cdot s^{-1}$ to 0.48 $m \cdot s^{-1}$. The results obtained show that the efforts to improve the equipment for the capture of particulate matter emissions are going in the right direction. The goal is to further optimize the shape of the charging electrodes, which we expect to intensify the corona discharge on the electrode surfaces at a lower supply voltage than before. The aim is to improve the protection of human health and quality of life by capturing particulate matter. It is expected that the supply voltage and, thus, the operating costs of the device will be reduced at the same time.

Author Contributions: J.D., investigation, conceptualization resources, writing—original draft; M.H., data curation, formal analysis, methodology, writing—review and editing, funding; N.Č.K., data curation and B.Č., formal analysis. All authors have read and agreed to the published version of the manuscript.

Funding: This publication has been produced with the support of the KEGA 032ŽU-4/2022—Implementation of Knowledge about Modern Ways of Reducing Environmental Burden in the Energy Use of Solid Fuels and Waste into the Pedagogical Process, VEGA 1/0233/19— Structural Modification of a Burner for the Combustion of Solid Fuels in Small Heat Sources and Grant System of University of Zilina No. 1/2021 (15899).

Institutional Review Board Statement: Not applicable.

Informed Consent Statement: Not applicable.

Data Availability Statement: Not applicable.

Conflicts of Interest: The funders had no role in the design of the study; in the collection, analyses, or interpretation of data; in the writing of the manuscript, or in the decision to publish the results. The authors declare no conflict of interest.

References

1. Singh, K.; Tripathi, D. Particulate matter and human health. *Environ. Health* **2021**. [CrossRef]
2. Giordani, J.; Concereggi, C.; Zarandiniova, E.; Pini, A.; Pini, L.; Piovanelli, P.; Ciarfaglia, M.; Tanucci, C. Characterization of the impact of particulate matter and fine particulate matter on asthma exacerbation 2020. In Proceedings of the Conference: 121° Congresso Nazionale-Società Italiana di Medicina Interna, Rome, Italy, 23–25 August 2021.
3. Harrison, R.M. Airborne particulate matter. *Philos. Trans. R. Soc. A Math. Phys. Eng. Sci.* **2020**, *378*, 20190319. [CrossRef] [PubMed]
4. Mizuno, A. Electrostatic precipitation. *IEEE Trans. Dielectr. Electr. Insul.* **2000**, *7*, 615–624. [CrossRef]
5. Sakuma, Y.; Yamagami, R.; Zukeran, A.; Ehara, Y.; Inui, T. Reduction of so2 and dpm using heat exchanger and electrostatic precipitation in diesel engine. *Mar. Eng.* **2014**, *49*, 533–538. [CrossRef]
6. Takasaki, M.; Kurita, H.; Kubota, T.; Takashima, K.; Hayashi, M.; Mizuno, A. Electrostatic precipitation of diesel PM at reduced gas temperature. In Proceedings of the Conference 2015 IEEE Industry Applications Society Annual Meeting, Addison, TX, USA, 18–22 October 2015. [CrossRef]
7. Ehara, Y.; Ohashi, M.; Zukeran, A.; Kawakami, K.; Inui, T.; Aoki, Y. Development of hole-type electrostatic precipitator. *Int. J. Plasma Environ. Sci. Technol.* **2017**, *11*, 9–12.
8. Sivak, P.; Taus, P.; Rybar, R.; Beer, M.; Simkova, Z.; Banik, F.; Zhironkin, S.; Citbajova, J. Analysis of the combined ice storage (pcm) heating system installation with special kind of solar absorber in an older house. *Energies* **2020**, *13*, 3878. [CrossRef]
9. Enviroportal.sk–Emisie znečisťujúcich látok do ovzdušia. Web Article. Last Update 2021. Online—26 April 2022. Available online: https://www.enviroportal.sk/indicator/detail?id=141 (accessed on 1 June 2022).
10. Trnka, J.; Jandačka, J.; Holubčík, M. Improvement of the standard chimney electrostatic precipitator by dividing the flue gas stream into a larger number of pipes. *Appl. Sci.* **2022**, *12*, 2659. [CrossRef]
11. Eom, Y.S.; Kang, D.H.; Choi, D.H. Numerical analysis of PM2.5 particle collection efficiency of an electrostatic precipitator integrated with double skin façade in a residential home. *Build. Environ.* **2019**, *162*, 106245. [CrossRef]
12. Gao, X.; Zheng, C.; Liang, C.; Liu, S.; Yang, Z.; Shen, Z.; Guo, Y.; Zhang, Y. Balance and stability between particle collection and re-entrainment in a wide temperature-range electrostatic precipitator. *Powder Technol.* **2018**, *340*, 173–179. [CrossRef]
13. Molchanov, O.; Krpec, K.; Horák, J. Electrostatic precipitation as a method to control the emissions of particulate matter from small-scale combustion units. *J. Clean. Prod.* **2019**, *246*, 119022. [CrossRef]
14. Caroll, J.; Finnan, J. Use of electrostatic precipitators in small-scale biomass furnaces to reduce particulate emissions from a range of feedstocks. *Biosyst. Eng.* **2017**, *163*, 94–102. [CrossRef]
15. Brunner, T.; Wuercher, G.; Obernberger, I. 2-Year field operation monitoring of electrostatic precipitators for residential wood heating systems. *Biomass Bioenergy* **2018**, *111*, 278–287. [CrossRef]
16. Ahmadi, M.; Berkhoff, A.P.; de Boer, A. Computational fluid dynamics approach to evaluate electrostatic precipitator performance. In Proceedings of the 2017 COMSOL Conference, Rotterdam, The Netherlands, 4–6 October 2017.
17. Haque, S.; Rasul, M.; Khan, M. Modelling and Simulation of Particle Trajectory Inside an Electrostatic Precipitator. *Computational Fluid Dynamics: Theory, Analysis and Applications.* Project: Performance Improvement of Electrostatic Precipitator: Aspects of Fine Particulate Emission Control 2013. Available online: https://www.researchgate.net/publication/266487837_MODELLING_AND_SIMULATION_OF_PARTICLE_TRAJECTORY_INSIDE_AN_ELECTROSTATIC_PRECIPITATOR/references (accessed on 1 June 2022).
18. Zhao, L.; Knight, M.; Zhu, H. Modelling and optimisation of a wire-plate ESP for mitigation of poultry PM emission using COMSOL. *Biosyst. Eng.* **2021**, *211*, 35–49. [CrossRef]
19. Skodras, G.; Kaldis, S.P.; Sofialidis, D.; Faltsi, O.; Grammelis, P.; Sakellaropoulos, G.P. Particulate removal via electrostatic precipitators—CFD simulation. *Fuel Processing Technol.* **2006**, *87*, 623–631. [CrossRef]
20. Zukeran, A.; Ito, K.; Tamura, R.; Kawada, Y.; Taoka, T. Simulation and measurement of charged particle trajectory with ionic flow in a wire-to-plate type electrostatic precipitator. *J. Electrotatics* **2020**, *107*, 103488. [CrossRef]
21. Yan, K.; Li, S.; Huang, Y.; Zheng, Q.; Deng, G. A numerical model for predicting particle collection efficiency of electrostatic precipitators. *Powder Technol.* **2019**, *347*, 145–148. [CrossRef]
22. Mohebbi, A.; Heidarbeig, M. CFD Modeling of Particulate Pollutants Removal by Electrostatic Precipitator (ESP). In Proceedings of the 8th International Chemical Engineering Congress & Exhibition (IChEC 2014), Kish, Iran, 24–27 February 2014.
23. Gou, B.; Zu, A.; Gou, J. Numerical Modelling of ESP for Design Optimization. *Procedia Eng.* **2015**, *102*, 1366–1372. [CrossRef]
24. Gou, X.; Zhang, Q.; Zhang, J. Improvement of Corona Discharge Model and Its Application on Simulating Corona Discharge in the Presence of Wind. *Math. Probl. Eng.* **2017**, *52*, 1–10. [CrossRef]
25. Everson, R.C.; Arif, S.; Arif, A.; Branken, D.J.; Neomahus, H.; Noras, M.; le Grange, L. An experimentally validated computational model to predict the performance of a single-channel laboratory-scale electrostatic precipitator equipped with spiked and wire discharge electrodes. *J. Electrotatics* **2021**, *112*, 103595. [CrossRef]
26. Dong, M.; Zhou, F.; Shang, Y.; Li, S. Numerical study on electrohydrodynamic flow and fine-particle collection efficiency in a spike electrode-plate electrostatic precipitator. *Powder Technol.* **2019**, *351*, 71–83. [CrossRef]
27. Dong, M.; Zhou, F.; Zhang, Y.; Shang, Y.; Li, S. Numerical study on fine-particle charging and transport behaviour in electrostatic precipitators. *Powder Technol.* **2018**, *330*, 210–218. [CrossRef]
28. Böhm, J. *Elektrické odlučovače*; Müszaki Könyvkiadó (MLR), SNTL–Nakladatelství technické literatury (ČSSR), Verlag Technik (NDR): Praha, Czech Republic, 1977; 327s.

29. Papučík, Š.; Jandačka, J.; Chabadova, J.; Pilát, P. Production of particulate matter from the combustion of wood pellets. *Eur. Phys. J. Conf.* **2015**, *92*, 02057. [CrossRef]
30. Skvarekova, E.; Tausova, M.; Senova, A.; Wittenberger, G.; Novakova, J. Statistical Evaluation of Quantities Measured in the Detection of Soil Air Pollution of the Environmental Burden. *Appl. Sci.* **2021**, *11*, 3294. [CrossRef]
31. Oplyne.info–Porovnanie základných zdrojov vykurovania z pohľadu investičných a prevádzkových nákladov. Last update 4/2021. Online—27 April 2022. Available online: https://www.oplyne.info/porovnanie-zakladnych-zdrojov-vykurovania/ (accessed on 1 June 2022).
32. Bologa, A.; Paur, H.R.; Woletz, K. Development and study of an electrostatic precipitator for small scale wood combustion. *Int. J. Plasma Environ. Sci. Technol.* **2011**, *5*, 168–173.